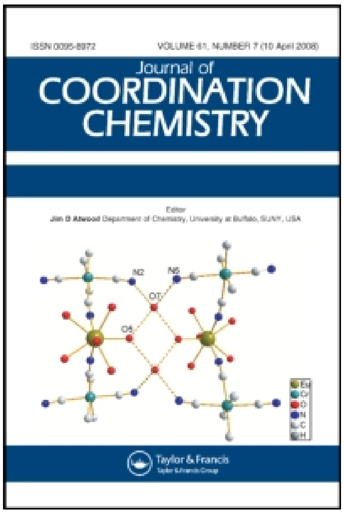

Journal of Coordination Chemistry
Publication details, including instructions for authors and subscription information:
http://www.informaworld.com/smpp/title~content=t713455674

Synthesis, characterization, potentiometric and thermodynamic studies of transition metal complexes with 1-benzotriazol-1-yl-1-[(<i>p</i> -methoxyphenyl) hydrazono]propan-2-one

Ali El-Dissouky[a]; Nadia M. Shuaib[a]; Nouria A. Al-awadi[a]; Alaa B. Abbas[a]; Ahmeda El-Sherif[a]
[a] Faculty of Science, Department of Chemistry, Kuwait University, Safat 13060, State of Kuwait

To cite this Article El-Dissouky, Ali , Shuaib, Nadia M. , Al-awadi, Nouria A. , Abbas, Alaa B. and El-Sherif, Ahmeda(2008) 'Synthesis, characterization, potentiometric and thermodynamic studies of transition metal complexes with 1-benzotriazol-1-yl-1-[(**<i>p</i>** -methoxyphenyl) hydrazono]propan-2-one', Journal of Coordination Chemistry, 61: 4, 579 — 594

To link to this Article: DOI: 10.1080/00958970701365492
URL: http://dx.doi.org/10.1080/00958970701365492

Journal of Coordination Chemistry
Vol. 61, No. 4, 20 February 2008, 579–594

Taylor & Francis
Taylor & Francis Group

Synthesis, characterization, potentiometric and thermodynamic studies of transition metal complexes with 1-benzotriazol-1-yl-1-[(*p*-methoxyphenyl) hydrazono]propan-2-one†

ALI EL-DISSOUKY*, NADIA M. SHUAIB, NOURIA A. AL-AWADI, ALAA B. ABBAS and AHMEDA EL-SHERIF

Faculty of Science, Department of Chemistry, Kuwait University, P. O. Box 5969, Safat 13060, State of Kuwait

(*Received 11 February 2007; in final form 14 February 2007*)

A new series of Mn^{2+} and Co^{2+} complexes with 1-benzotriazol-2-yl-1-[(*p*-methoxyphenyl)-hydrazono]propan-2-one (BMHP) were synthesized and characterized by the elemental analysis, magnetic and different spectral techniques. Proton dissociation constant of the free ligand and the stepwise stability constants of its metal complexes were determined potentiometrically in 0.1 M KC1 and 40% (v/v) ethanol–water. The dissociation constants of the free ligand and its metal complexes were determined at different temperatures and the corresponding thermodynamic parameters were calculated and discussed. The dissociation process was found to be non-spontaneous, endothermic and entropically unfavorable. The changes in the standard ΔG^0 and ΔH^0 accompanying complexation were decreased with increasing metal ionic radius but increased with increasing electronegativity, ionization enthalpy, and hydration enthalpy of the metal ion. The values of $(-\Delta G^0)$ and $(-\Delta H^0)$ were in the order: $Mn^{2+} < Co^{2+} < Ni^{2+} < Cu^{2+}$, in accord with the Irving-Williams order. The complexes were found to be stabilized by both enthalpy and entropy changes and the results suggest that complexation is an enthalpy-driven process. The distribution diagrams of the complexes in solution were evaluated.

Keywords: Benzotriazole; Complexes; Spectra; Thermodynamics

1. Introduction

Hydrazones and their derivatives are of interest for coordination behavior [1] and wide biological activities. For example, ferimzone can prevent and cure cercospora oryzae, helminthosporinm oryzae and piricularia oryzae [2]. Also they possess anti-inflammatory, analgesic antipyretic, antibacterial and antitumor [6–19] activities. Furthermore, the metal complexes of hydrazones have gained attention due to their biological activity and ability to act as inhibitors for many enzymes [3–5]. Triazole and its derivatives have been patented and extensively employed in agriculture [21].

*Corresponding author. Email: adissouky@yahoo.com
†Presented at the 37th International Conference of Coordination Chemistry (37th ICCC), Cape Town, 13–18 August, 2006.

Journal of Coordination Chemistry
ISSN 0095-8972 print/ISSN 1029-0389 online © 2008 Taylor & Francis
DOI: 10.1080/00958970701365492

Triazole derivatives are known to exhibit anti-inflammatory [13, 14], antiviral [15], analgesic [16], antimicrobial [17–19], anticonvulsant [18, 19] and antidepressant activity [20]. They also act as chelating agents for a large number of metal ions giving complexes with very interesting stereochemistry, electrochemistry and magnetic behavior. The synthesis and characterization of some metal complexes with triazole-based ligands [21, 22] gave complexes with different structure depending on the metal salt used and the reaction conditions. In continuation of our interest in studying the ligating behavior of such compounds, we synthesize and characterize solid complexes of a ligand containing both the triazole and hydrazone moieties, (1-benzotriazol-1-yl-[(*p*-methoxyhphenyl)-hdrazono] propan-2-one) (BMHP), with Mn^{2+}, Co^{2+}, Ni^{2+} and Cu^{2+}. The thermodynamic properties were also determined and discussed. Such work may be relevant to interactions occurring in biological systems, such as metal-protein and metal-nucleic acid interactions.

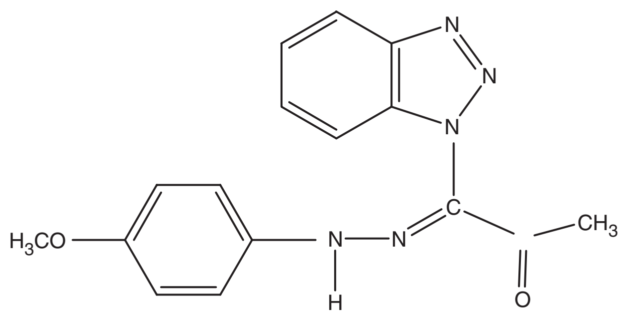

BMHP

2. Experimental

2.1. *Reagents and materials*

All metal salts, NaN_3, NH_4SCN, $(NH_4)_2S_2O_8$, and solvents were purchased from Aldrich and used without further purification. $Hg[Co(NCS)_4$ was obtained as a calibrant from Sigma Aldrich chemical company.

2.2. *Synthesis of the organic ligand*

The organic ligand was synthesized according to the method reported [23].

2.3. *Synthesis of the metal complexes*

The synthesis of cobalt(II) and manganese(II) complexes were carried out under nitrogen.

Copper(II) and nickel(II) complexes. These complexes were prepared and characterized as described previously [21, 22].

Manganese complexes:

$[Mn(HL)_2](ClO_4)_2$ (1). The complex was synthesized by the addition of methanolic solution (30 mL) of $Mn(ClO_4)_2 \cdot 6H_2O$ (10 mmol) to deaerated solution (25 mL) of HL

(35 mmol) in the same solvent. The reaction mixture was stirred at room temperature for 3h under N_2. The brown solid formed was filtered off, washed several times with MeOH and Et_2O and dried under vacuum over P_4O_{10}.

[Mn(HL)$_2$(OAc)$_2$] (2). The acetato-complex was prepared as described for the synthesis of **1** but using $Mn(OAc)_2 \cdot H_2O$ instead of $Mn(ClO_4)_2 \cdot 6H_2O$. Treatment of the reaction mixture with NaOH solution leads to the formation of a green amorphous solid insoluble in most solvents; elemental analysis indicates a mixture of different products. Attempts to recrystallize or isolate the different components failed.

[MnL$_2$(H$_2$O)$_2$]OAc (3). To a solution of HL (35 mmol) in methanol (20 mL), a solution of 10 mmol $Mn(OAc)_2 \cdot H_2O$ in MeOH (30 mL) was added under stirring at room temperature without N_2. After 15 min, an aqueous NaOH solution (40 mmol in 5 mL H_2O) was added. The stirring was continued for another 4 h during which a green solid was isolated. The solid formed was then filtered off, washed with MeOH and Et_2O and dried under vacuum over P_4O_{10}.

Cobalt complexes

[Co(HL)$_2$](ClO$_4$)$_2$ (4). A solution of $Co(ClO_4)_2 \cdot 6H_2O$ (10 mmol) in EtOH (30 mL) was added to a deaerated solution of HL (25 mmol) in the same solvent (25 mL) under N_2. The reaction mixture was stirred for 30 min at room temperature. The bluish green solid formed was filtered off, washed several times with EtOH followed by Et_2O and dried under vacuum over P_4O_{10}.

[Co(HL)$_2$Cl$_2$]Cl (5). A solution of $CoCl_2 \cdot H_2O$ (10 mmol) in EtOH (30 mL) was added to a solution (30 mL) of HL (25 mmol) in the same solvent, followed by addition of $(NH_4)_2S_2O_8$ (20 mmol) in EtOH–H_2O mixture (1 : 1, v/v), (30 mL). The reaction mixture was refluxed on a water bath for 3 h and filtered hot to remove any unreacted oxidizing agent. The filtrate was evaporated under reduced pressure to half of its volume and left to cool in a refrigerator. The brown solid isolated was filtered off, washed with EtOH–H_2O (1 : 1, v/v) followed by Et_2O and dried under vacuum over P_4O_{10}.

[Co(HL)$_2$Cl$_2$]X, X = SCN or N$_3$ (6, 7, respectively). These complexes were synthesized by mixing equimolar amounts of $[Co(HL)_2Cl_2]Cl$ and NH_4SCN or NaN_3 in EtOH–H_2O mixture (1 : 1, v/v), 60 mL) and the reaction mixture was stirred for 10–15 min for complete reaction. The green solid was filtered off, washed several times with EtOH followed by Et_2O and dried in vacuum over P_4O_{10}.

2.4. *Preparation of solutions*

Metal ion solutions (2.00×10^{-4} M) were prepared from Analar metal chloride in doubly distilled water and standardized with EDTA [24] and atomic absorption. The ligand solution (1.00×10^{-3} M) was prepared by dissolving an accurate mass of the solid in purified ethanol (absolute). A solution of 0.10 M KC1 was also prepared in doubly distilled water. A carbonate-free sodium hydroxide solution in 40% (v/v) ethanol–water mixture was used as a titrant after standardization against standard oxalic acid solution.

2.5. *Apparatus and procedures for the potentiometric titrations*

Apparatus, general conditions and methods of calculation were the same as in previous studies [25, 26]. The following mixtures (i–iii) were prepared and titrated potentiometrically at 298 K against standard 1.00×10^{-2} M NaOH in 40% (v/v) ethanol–water:

(a) 5.00 mL 1.00×10^{-2} M HC1 + 5.00 mL of 0.10 M KC1 + 20 mL ethanol.
(b) 5.00 mL 1.00×10^{-2} M HC1 + 5.00 mL 0.10 M KC1 + 15.00 mL ethanol + 5.00 mL 1.00×10^{-3} M ligand.
(c) 5.00 mL 1.00×10^{-2} M HC1 + 5.00 mL 0.10 M KC1 + 15.00 mL ethanol + 5.00 mL 1.00×10^{-3} M ligand + 5.00 mL 2.00×10^{-4} M metal ion.

The volume of each mixture was increased to 50.00 mL with doubly distilled water before titration. These titrations were repeated at 308 and 318 K. Temperature was kept constant within ±0.05 K by using an ultrathermostat (Galenkamp thermostirrer 85). The pH measurements were carried out using VWR Scientific instruments model 8000 pH-meter accurate to ±0.01 units. The pH-meter readings in 40% (v/v) ethanol–water mixture are corrected according to the method of Van Uitert and Hass [27]. The concentration distribution diagrams were obtained using the program SPECIES [28].

2.6. *Physical measurements and analysis*

CHN analyses were obtained using LECO-CHNS 932 Analyzer. FT-IR spectra were recorded as KBr discs with a Schimadzu 2000 FT-IR spectrophotometer. Electronic spectra were accomplished on a Cary Varian 5 UV/Vis spectrophotometer. The room temperature magnetic susceptibility measurements for the complexes were determined by the Gouy balance using $Hg[Co(NCS)_4]$ as calibrant. The room temperature X-band ESR spectra were recorded for polycrystalline and DMF samples in the presence of DPPH as a standard utilizing an ECS 106 ESR spectrometer. The molar conductances of the complexes were measured for 1.00×10^{-3} M DMSO solutions at $25 \pm 1°C$ using a Jenway 4020 conductivity meter.

3. Results and discussion

3.1. *General and molar conductivity*

All complexes are air stable and insoluble in most organic solvents and water but freely soluble in coordinating solvents such as pyridine, picolines, DMF or DMSO. All have higher m.p. or decomposition points than the parent ligand.

The conductivity values of the complexes as 10^{-3} M DMSO solution at $25 \pm 1°C$, table 1, indicate the 1 : 2 electrolytic nature of $[Mn(HL)_2](ClO_4)_2$ and $[Co(HL)_2](ClO_4)_2$; 1 : 1 of $[MnL_2(H_2O)_2]OAc$ and $[Co(HL)_2Cl_2]X$, X = Cl, SCN or N_3 and that $[Mn(HL)_2(OAc)_2]$ is a non-electrolyte [29, 30].

Table 1. Elemental analysis {% found (% calculated)}, color, room temperature, molar conductivity ($\Omega^{-1}\,cm^2\,mol^{-1}$) and room temperature magnetic moment values (B.M.) for the complexes.

Complex	Color	Λ_M	μ_{eff}	(%) C	(%) H	(%) N
$[Mn(HL)_2](ClO_4)_2$	Brown	152.61	5.63	44.5(44.0)	3.5(3.4)	16.0(16.1)
$[Mn(HL)_2(OAc)_2]$	Brownish red	4.98	5.92	54.2(54.6)	4.8(4.6)	17.6(117.7)
$[MnL_2(H_2O)_2]OAc$	Green	63.78	4.83	53.1(53.3)	4.3(4.6)	18.1(18.3)
$[Co(HL)_2](ClO_4)_2$	Bluish-green	156.97	4.53	44.1(43.8)	3.5(3.4)	15.7(16.0)
$[Co(HL)_2Cl_2]Cl$	Brownish green	81.09	Diamagnetic	48.6(49.0)	3.6(3.8)	18.3(17.9)
$[Co(HL)_2Cl_2]SCN$	Green	77.89	Diamagnetic	48.8(49.1)	3.6(3.7)	18.8(19.1)
$[Co(HL)_2Cl_2]N_3$	Green	73.78	Diamagnetic	48.9(48.6)	4.0(3.8)	22.8(23.0)

3.2. *Infrared spectra*

The FT-IR spectral data of the ligand were reported previously [21, 22]. The characteristic IR bands (cm^{-1}) at 3200–3290, $\upsilon_{(NH)}$, 1680 $\upsilon_{(C=O)}$, 1602 $\upsilon_{(C=N)}$ are in a good agreement with structure I for the free ligand. The IR spectra of the newly synthesized complexes of manganese and cobalt are recorded in the region of 200–4000 cm^{-1} and tentative assignments are given in table 2. Spectra of $[Co(HL)_2Cl_2]X$, X = SCN exhibit bands at 2055 and 760 cm^{-1} due to $\upsilon(C\equiv N)$ and $\upsilon(C–S)$, respectively, characteristic of ionic SCN. The spectrum for $X = N_3$ displays a strong absorption at 2035 cm^{-1} characteristic of ionic azide [31]. The spectra of the three complexes exhibit a new weak-medium band at 266–268 cm^{-1} characteristic of $\upsilon(Co–Cl)$. The appearance of only one band characteristic of the chloride suggests that the two chloride ions are equivalent. The spectra of all complexes display broad bands with medium-strong intensity at 3220–3335 cm^{-1} due to $\upsilon(NH)$. In all complexes, these bands are red shifted with respect to that of the ligand (3245–3418 cm^{-1}) supporting their bonding to the metal. The spectrum of $[MnL_2(H_2O)_2]OAc$ displays a broad medium band at 3480 cm^{-1} which is absent in all other complexes. Based on the elemental analysis and the conductivity data, this could be assigned to coordinated water molecules, supported by the appearance of new weak bands at 825, 580 and 489 cm^{-1} characteristic of coordinated water molecules [31]. The spectra of $[Mn(HL)_2](ClO_4)_2$ and $[Co(HL)_2](ClO_4)_2$ display two bands at 1098–1100 and 628–632 cm^{-1} indicative of non-coordinated perchlorate [31]. The spectrum of $[Mn(HL)_2(OAc)_2]$ displays a medium-strong band at 1569 and medium at 1353 cm^{-1} with $\Delta\upsilon = 216\,cm^{-1}$ characteristic of monodentate coordinated acetate group. The spectrum of $[MnL_2(H_2O)_2]OAc$ exhibits a new strong band at 1618 cm^{-1} characteristic of ionic acetate. The spectra of all complexes except $[MnL_2(H_2O)_2]OAc$, display bands at 1649–1672, 1577–1588 cm^{-1} due to $\upsilon(C=O)$ and $\upsilon(C=N)$, respectively. These bands appeared at lower wavenumbers than in the free ligand (1680 and 1602 cm^{-1}, respectively) indicating their bonding to the metal ions. The spectrum of $[MnL_2(H_2O)_2]OAc$ exhibits two bands at 1449 and 1390 cm^{-1} which are assigned to $\upsilon(C–O)$ and $\upsilon(N=N)$, respectively, indicating bonding of the ligand to the metal via the deprotonated enolato oxygen and azo nitrogen atoms. Accordingly the ligand is neutral and monobasic bidentate. The far IR spectra of all complexes display bands characteristic of $\upsilon(M–O)_L$ and $\upsilon(M–N)_L$, L = ligand, at 500–522 and 412–470 cm^{-1} and $\upsilon(M–O)_X$, $X = H_2O$ or OAc, at 540 and 536 cm^{-1} supporting the assumption of N,O coordination by the ligand.

Table 2. The IR spectra (υ, cm^{-1}) of the complexes.[a]

Complex	υ(NH, H_2O)[b]	υ(C=O)	υ(N=N)	υ(C=N)	υ(M–O)	υ(M–N)	υ(M–Cl)	υ(X)[a]
$[Mn(HL)_2](ClO_4)_2$	3285, 3310	1655s	–	1586s	500w	418w	–	1100vs, 628 m-w
$[Mn(HL)_2(OAc)_2]$	3245, 3295	1649m-s	–	1579m	522w, 540w	412w	–	1569s, 1353m
$[MnL_2(H_2O)_2]OAc$	3220, 3480	1446m	1390m		502w, 536w	426w	–	825, 580, 489, 1618s
$[Co(HL)_2](ClO_4)_2$	3290, 3318	1672s	–	1585m	509w	453w, 468w	–	1098vs, 632m
$[Co(HL)_2Cl_2]Cl$	3288, 3325	1669s	–	1577m	506w	450w, 704w	268w-m	–
$[Co(HL)_2Cl_2]SCN$	3285, 3335	1672s	–	1583s	511w	455w, 473w	266w-m	2055vs, 760 m
$[Co(HL)_2Cl_2]N_3$	3285, 3315	1672s	–	1588s	510w	455w, 470w	268w	2035s

[a]Diagnostic IR bands of the polyatomic ions or coordinated water. [b]Broad bands.

Table 3. The electronic spectral (cm^{-1}) data of manganese and cobalt complexes.

Complex	d–d transitions	$n-\pi^*$	$\pi-\pi^*$	$10D_q$	B	β	C
$[Mn(HL)_2](ClO_4)_2$	21,735, 24,385, 25,850	458, 31,576	40,366				
$[Mn(HL)_2(OAc)_2]$	18,080, 22,468, 25,176	29,330, 30,500	38,688	8580	694	0.81	2230
$[MnL_2(H_2O)_2]OAc$	19,600, 15,586	30,280	40,545				
$[Co(HL)_2](ClO_4)_2$	7600, 15,650, 16,100, 19,000	28,650, 30,600	39,670	4428	669	0.69	
$[Co(HL)_2Cl_2]Cl$	10,220, 14,900, 19,850, 28,680	31,285, 32,850	38,690	24,660	581		4817
$[Co(HL)_2Cl_2]SCN$	10,230, 14,860, 19,850, 28,700	31,000, 32,575	39,000	24,600	579		4810
$[Co(HL)_2Cl_2]N_3$	10,235, 14,855, 19,870, 28,800	31,100, 32,600	390,100	24,660	577		4812

3.3. *Magnetic and spectral studies*

3.3.1. Manganese complexes. The room temperature magnetic moment of $[Mn(HL)_2](ClO_4)_2$ and $[Mn(HL)_2(OAc)_2]$, table 3, are characteristic for an isolated $S = 5/2$ manganese(II) monomer [32, 33]. The electronic spectra of $[Mn(HL)_2](ClO_4)_2$ as nujol mull and MeCN solution are similar indicating the stability of this complex in solution. The spectra display bands of low intensity at 25,850, 24,385 and 21,735 cm^{-1} due to ${}^6A_1 \rightarrow {}^4E(D)$, ${}^6A_1 \rightarrow {}^4T_2(D)$ and ${}^6A_1 \rightarrow {}^4E$ transitions, respectively, for manganese(II) in a tetrahedral ligand field [34–37].

The X-band ESR spectra of $[Mn(HL)_2](ClO_4)_2$ either in the solid state or as MeCN solution at room temperature are similar with an isotropic spectrum of six lines with spacing, A, of 82 G. The value of g obtained from the spectrum is 2.0. The low A-value with the high μ_{eff}. at room temperature support tetrahedral structure of the complex [36, 37].

The electronic spectrum of $[Mn(HL)_2(OAc)_2]$ either as nujol mull or DMF solution displays bands with low intensity at 18,080, 22,950 and 25,986 cm^{-1}. The ground state of high spin octahedral manganese(II) is ${}^6A_{1g}$ and there is no other terms of sextet spin multiplicity. Therefore, all d–d transitions are Laport and spin forbidden [38]. The excited states for d^5 configuration are ${}^4G$, ${}^4D$ and ${}^4P$ in the order of increasing energy. Accordingly, the spectral bands are assigned to ${}^6A_{1g} \rightarrow {}^4T_{1g}({}^4G)$, ${}^6A_{1g} \rightarrow {}^4T_{2g}({}^4G)$, ${}^6A_{1g} \rightarrow {}^4E_g$, ${}^4A_{1g}({}^4G)$ transitions, respectively. Furthermore, the broad nature and the position of the band at 22,950 cm^{-1} is typical of octahedral manganese(II) complexes. The non-broad nature of the other two transitional bands indicates that the vibronic coupling or the spin orbit coupling do not raise the degeneracy of the terms concerned [39–41]. The values of the ligand field parameters B, C, D_q and β are calculated [35, 42] and given in table 3. The metal-ligand bond covalency could be evaluated from the value of $\beta = B/B_o$, where B_o for the free manganese(II) $= 860\,cm^{-1}$ [33, 43]. The value of β indicates that the manganese-ligand bonding is mainly ionic.

The X-band ESR spectrum of polycrystalline $[Mn(HL)_2(OAc)_2]$ at 300 K displays only a broad line with $g = 2.14$, attributed to dipolar–dipolar interaction and enhanced spin-lattice relaxation. The DMF solution spectrum at 298 K exhibits a six line hyperfine pattern at $g = 2.004$ indicating the absence of spin-orbit coupling in the ground ${}^6A_{1g}$ state. The hyperfine spectrum of these six lines is due to the electron spin-nuclear spin coupling and corresponds to $m_I \pm 5/2$, $\pm 3/2$, $\pm 1/2$, resulting from the allowed transitions ($\Delta m_s = \pm 1$ and $\Delta m_I = 0$). The hyperfine constant value was found to be 108 G which is larger than that observed for the tetrahedral complex $[Mn(HL)_2](ClO_4)_2$ and is consistent with octahedral manganese(II) complexes.

The effective moment of $[MnL_2(H_2O)_2]OAc$ at 300 K of 4.83 B.M. is very close to the spin only value (4.90 B.M.) as expected for high spin magnetically dilute d^4 ($S = 2$) [43].

The electronic spectrum of the complex in MeCN as a solvent and as a nujol mull are similar and exhibit two intense bands at 30,280, 23,810, and two broad bands at 19,600 and 15,586 cm^{-1} with ε_{max} 12,405, 4085, 668 and 298 M^{-1} cm^{-1}, respectively. The broad bands at 19,600 and 15,586 cm^{-1} are similar to those reported for a distorted octahedral manganese(III) complexes and could be assigned to the $xy \rightarrow z^2$ and $xz(yz) \rightarrow z^2$ transitions, respectively [44]. The band at 23,810 cm^{-1} is ascribed to a ligand to metal charge transfer transition probably from the ligand oxygen to $3d(Mn^{3+})$. The band at 30,280 cm^{-1} could be associated with the $n - \pi^*$ transition. The higher energy band at 40,545 cm^{-1} is assigned to π–π^* transition.

3.3.2. Cobalt complexes. The room temperature magnetic moment value for $[Co(HL)_2](ClO_4)_2$ of 4.53 B.M is characteristic for high spin d^7 tetrahedral complexes, while the complexes $[Co(HL)_2Cl_2]X$, $X = Cl$, SCN or N_3 are diamagnetic in accordance with the $^1A_{1g}$ ground state for low spin d^6 configuration [45, 46].

The electronic spectrum of $[Co(HL)_2](ClO_4)_2$ displays intense bands at 7600, 15,650, 16,100 and 19,000 cm^{-1}, table 3. The spectral shape and the band positions are characteristic of a pseudo-tetrahedral cobalt(II) complexes [35, 47, 48]. The bands at 15,650 and 16,100 cm^{-1} are components of a composite band (υ_3) due to the interaction with the doublet state through spin-orbit coupling and could be attributed to the $^4A_2 \rightarrow {}^4T_1(P)$ transition [4, 16, 17]. The lower energy band is therefore attributed to the spin allowed, υ_2 $^4A_2 \rightarrow {}^4T_1(F)$ transition. The ligand field parameters calculated and given in table 3 are comparable to the values reported for tetrahedral cobalt(II) complexes with N_2O_2 chromophores.

The X-band ESR spectrum of this complex at 300 K exhibits a broad line due to the rapid relaxation of cobalt(II). Analysis of the spectrum gave $g_{\parallel} = 3.95$ and $g_{\perp} = 1.98$. The large deviation of the average g-value (2.64) from the spin only value (2.0023) could be attributed to the large angular momentum contribution.

The electronic spectra of $[Co(HL)_2Cl_2]X$, $X = Cl$, SCN or N_3, table 3, as nujol mull or MeCN solution are similar and exhibit bands similar to those reported for octahedral cobalt(III) complexes. These bands could be assigned to $^1A_{1g} \rightarrow {}^3T_{1g}$, $^1A_{1g} \rightarrow {}^3T_{2g}$, $^1A_{1g} \rightarrow {}^1T_{1g}$ and $^1A_{1g} \rightarrow {}^1T_{2g}$ transitions according to the increasing energy. The splitting of the $^1T_{1g}$ into two bands could be taken as evidence for trans structure of these complexes. The different ligand field parameters are calculated and given in table 3.

3.4. *Equilibrium study*

3.4.1. Ligand dissociation constant. In order to calculate the stability constants of metal chelates, the acid dissociation constant of BMHP was first determined from titration curves for HCl in the presence and absence of BMHP. The average number of protons associated with the BMHP at different pH values, $\bar{n}_A$ was calculated according to Irving and Rossotti [49]. Thus, the formation curve (n_A *vs.* pH) for the proton-ligand systems were constructed and found to extend between 0 and 1 in the $\bar{n}_A$ scale. This means that BMHP has one dissociable proton. Different computational methods [50] were applied to evaluate the dissociation constant, table 4. The values of pK at different temperature

Table 4. Thermodynamic parameters of dissociation of free ligand in 40% (v/v) ethanol–water mixture in the presence of 0.1 M KCl at different temperatures.

T (K)	pK_1	ΔG_1^0 (kJ mol^{-1})	ΔH^0	$T\Delta S_1^0$
298	10.20 ± 0.06	58.20		
308	10.04 ± 0.05	59.21	28.12	−31.09
318	9.89 ± 0.05	60.22		

indicate the ionization of the hydrazo proton rather than the enolato proton The number of replicates are three and the average values obtained are listed in table 4.

3.4.2. Metal-ligand stability constants. Stability constants of metal complexes were measured potentiometrically by knowing the ligand pK_a and the effect of metal ion on the ligand titration curve. The formation curves for the metal complexes were obtained by plotting the average number of ligands attached per metal ions (n) (calculated according to Irving and Rossotti [49]); *versus* the free ligand exponent (pL). These curves were analyzed and the successive stability constants were determined using different computational methods [51, 52] agreeing within 1%; average values are given in table 5. The following general observations pertain:

(a) The maximum value of $\bar{n}$ of 2, indicates the formation of 1 : 1 and 1 : 2 (metal : ligand) complexes in solution while in solid state only 1 : 2 and 1 : 3 species are isolated.
(b) The very low concentration of metal ion solution used in the present study (2.00×10^{-5} M) prevents the possibility of formation of polynuclear complexes [25, 26].
(c) The metal titration curves are displaced to the right-hand side of the ligand titration curve along the volume axis, indicating a proton release upon complex formation, further evidence for strong metal–ligand bonding.
(d) At the end of the titration, a change of color of the solution was observed without formation of a precipitate indicating complex formation.
(e) At constant temperature, the stability of the chelates increases in the order of: $Cu^{2+} > Ni^{2+} > Co^{2+} > Mn^{2+}$ [53, 54]. This order largely reflects the changes in the heat of complex formation across the series from a combination of the influence of both the polarizing ability of the metal ion [55] and the crystal field stabilization energies [56].
(f) All calculations of the stability constants are done at low pH. Therefore, the formation of hydroxo species e.g. [ML(OH)] or $[MS_{x-1}(OH)]^+$, where L is the ligand, S is the solvent molecule and X is the number of solvent molecules bound) could be ruled out.
(g) Table 5 shows that ($\log K_1 - \log K_2$) values are usually positive, since the coordination sites of the metal ions are more freely available for binding of the first molecule than the second one. The difference lies within 1.4 to 2.9 log units, revealing the importance of electrostatic and steric effects resulting from the addition of the second ligand, since the statistical effect contributes only 0.68 log units [52].

3.4.3. Effect of temperature. The pK_a for BMHP as well as the stability constants of its complexes with Mn^{2+}, Co^{2+}, Ni^{2+} and Cu^{2+} have been evaluated at 298, 308 and

Table 5. Stepwise stability constants for the complexation of free ligand with 3d divalent metal ions in 40% (v/v) ethanol–water mixture in the presence of 0.10 M KCl at different temperatures.

	$\log K_1$			$\log K_2$			$\log K_1 - \log K_2$		
Metal ion	298 K	308 K	318 K	298 K	308 K	318 K	298 K	308 K	318 K
Mn^{2+}	7.35 ± 0.04	7.18 ± 0.03	7.05 ± 0.04	5.73 ± 0.04	5.64 ± 0.03	5.52 ± 0.04	1.62	1.54	1.53
Co^{2+}	7.71 ± 0.03	7.55 ± 0.04	7.37 ± 0.05	6.02 ± 0.05	5.96 ± 0.05	5.80 ± 0.04	1.69	1.59	1.57
Ni^{2+}	8.06 ± 0.03	7.89 ± 0.05	7.72 ± 0.04	6.09 ± 0.03	5.99 ± 0.04	5.87 ± 0.04	1.97	1.9	1.85
Cu^{2+}	8.29 ± 0.03	8.19 ± 0.04	7.94 ± 0.04	6.64 ± 0.05	6.55 ± 0.03	6.39 ± 0.04	1.65	1.60	1.55

318 K, tables 4, 5. The enthalpy change (ΔH^0) for the dissociation or complexation process was calculated from the slope of the plot (pK_a or $\log K$ *vs.* $1/T$) using the graphical representation of the van Hoff equation (1) or (2)

$$-2.303RT \log K = \Delta H^0 - T\Delta S^0 \tag{1}$$

or

$$\log K = -\left(\frac{\Delta H^0}{2.303R}\right)\left(\frac{1}{T}\right) + \frac{\Delta S^0}{2.303R} \tag{2}$$

The free energy change (ΔG^0) could be calculated by using equation (3)

$$\Delta G^0 = -2.303RT \log K \tag{3}$$

from the values of ΔH^0 and ΔG^0, ΔS^0 could be calculated by equation (4)

$$\Delta S^0 = \left(\frac{\Delta H^0 - \Delta G^0}{T}\right) \tag{4}$$

where the gas constant $R = 8.314\,\mathrm{J\,K^{-1}\,mol^{-1}}$, K is the dissociation constant for the ligand or the stability constant of the complex, and T is the absolute temperature. The calculated thermodynamic functions are recorded in table 6. The positive ΔH^0 for the dissociation follows the general pattern for ionization processes [57]. The negative ΔS^0 indicates that the total number of solvent molecules bound to the ionized ligand is greater than that originally bonded to the neutral form.

The stepwise stability constants of the complexes formed at different temperatures were calculated and the average values are given in table 5. These values decrease with increasing temperature, confirming that the complexation process is more favorable at lower temperatures. The thermodynamic parameters of metal complexes, table 6, were calculated by a procedure similar to that used for the dissociation of BMHP. The divalent metal ions exist in solution as octahedrally hydrated species [53] and the obtained values of ΔH and ΔS can then be considered as the sum of two contributions: (a) release of H_2O molecules and (b) metal-ligand bond formation.

From these results the following conclusions can be made.

(1) All values of ΔG^0 for complexation are negative, indicating that chelation proceeds spontaneously.
(2) The negative values of ΔH^0 show that the chelation process is exothermic, indicating that the complexation reactions are favored at low temperatures. Furthermore, when a coordinate bond between the ligand and the metal ion is

Table 6. Thermodynamic parameters for ML and ML_2 complexes of free ligand with 3d divalent metal ions in 40% (v/v) ethanol–water mixture in the presence of 0.1 M KCl at different temperatures.

Metal ion	$-\Delta G_1^0$ 298 K	$-\Delta G_1^0$ 308 K	$-\Delta G_1^0$ 318 K	$-\Delta G_2^0$ 298 K	$-\Delta G_2^0$ 308 K	$-\Delta G_2^0$ 318 K	$-\Delta H_1^0$ 308 K	$-\Delta H_2^0$ 308 K	$T\Delta S_1^0$ 308 K	$T\Delta S_2^0$ 308 K
Mn^{2+}	41.93	42.34	42.92	32.69	33.26	33.60	27.25	19.02	15.09	14.24
Co^{2+}	43.99	44.52	44.99	34.35	35.14	35.31	29.01	19.85	15.51	15.29
Ni^{2+}	45.99	46.53	47.01	34.75	35.32	35.74	30.84	19.93	15.69	15.39
Cu^{2+}	47.30	47.94	48.35	48.35	38.51	38.91	31.71	22.63	16.23	15.88

formed, the electron density on the metal ion generally increases. Consequently, its affinity for a subsequent ligand molecule decreases, leading to an increase in ΔG^0 and ΔH^0 of complexation.

(3) It is generally noted that $-\Delta G_1^0 > -\Delta G_2^0$ and $-\Delta H_1^0 > -\Delta H_2^0$, table 6. This may be attributed to the steric hindrance produced by the entrance of a second molecule and charge neutralization. The electrostatic attraction in the ML complex is more than that in the ML_2 complex because ML is formed by interaction of the dipositively charged metal ion and mononegatively charged ligand, while the ML_2 complex is formed by the interaction of monopositively charged ML complex with another mononegatively charged ligand.

(4) ΔS^0 values for all investigated complexes are positive, indicating that the increase in entropy by the release of bound solvent molecules on chelation is greater than the decrease resulting from chelation itself, primarily because solvent molecules arranged in an orderly fashion around the ligand and the metal ion acquired a more random configuration on chelation. This could be referred to as configurational entropy.

3.4.4. Species distribution curves. Estimation of equilibrium concentrations of metal(II) complexes as a function of pH provides a useful picture of metal ion bonding in solution. All of the species distributions were calculated utilizing the Species Program [28]. The concentrations of complexes increase with increasing pH, figure 1. The species distribution pattern for Co(BMHP) complex, taken as representative of metal ligand complexes, is given in figure 1(a) Co(BMHP) complex starts to form at pH ~ 4.6 and reaches its maximum concentration (68%) at pH ~ 7.6, while $Co(BMHP)_2$ reaches a maximum concentration (98%) at pH ~ 10.6.

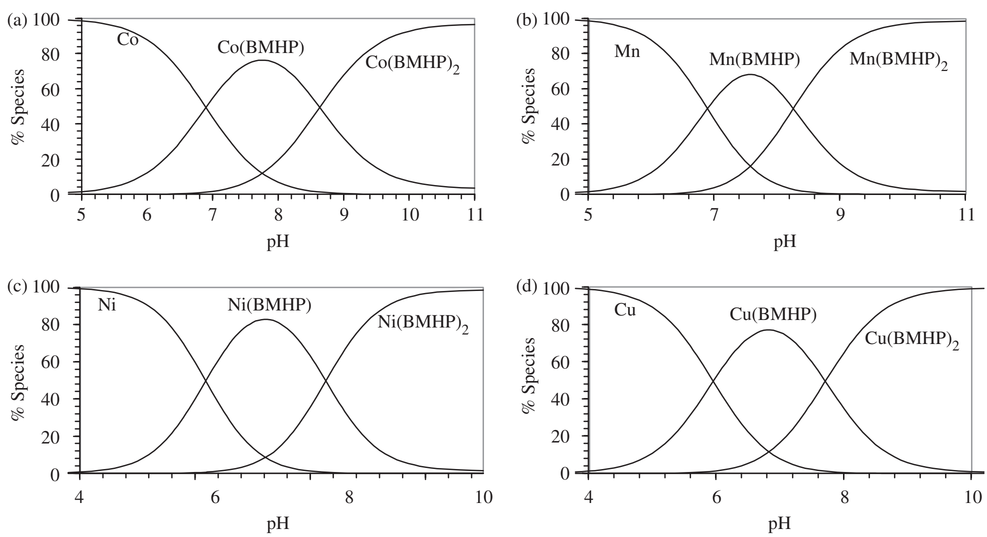

Figure 1. Distribution diagram of the various species in the binary systems: (a) [Co-BMHP], (b) [Mn–BMHP], (c) [Ni–BMHP] and (d) [Cu–BMHP] as a function of pH.

3.4.5. Variation of the thermodynamic functions of complexation with the properties of the metal ions. In an attempt to explain why a given ligand prefers binding to one metal rather than another, it is necessary to correlate the stability constants with the ionic radius, ionization enthalpy, hydration enthalpy, and the electronic configuration characteristic of the metal ion.

The overall ΔG^0 and ΔH^0 for the formation of Cu^{2+}, Ni^{2+}, Co^{2+} and Mn^2 complexes with BMHP are correlated with the reciprocal value of the metal ionic radius, figure 2, the total ionization enthalpy at 25°C for the process $M(gas) \rightarrow M^{2+}(gas) + 2e^-$ (figure 3), and enthalpy of hydration ΔH_H, (figure 4). The latter correlation

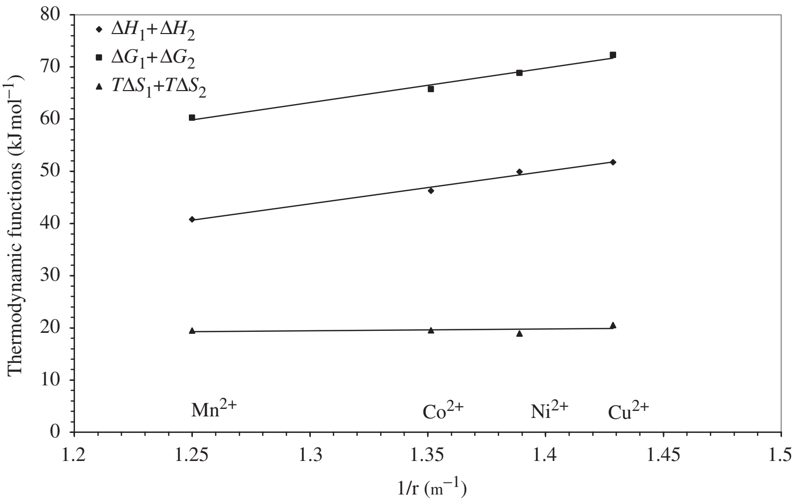

Figure 2. Variation of the overall thermodynamic functions at 308 K for BMHP complexes with the reciprocal value of the divalent metal ions the radii.

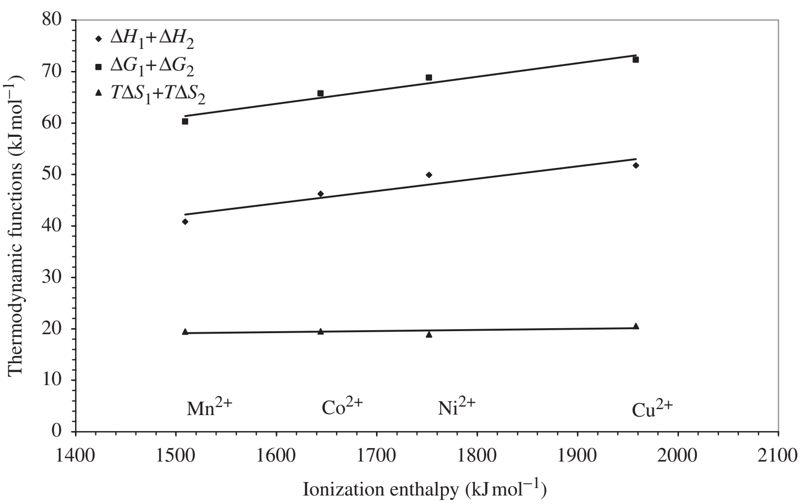

Figure 3. Variation of the overall thermodynamic functions at 308 K for BMHP complexes with the ionization enthalpy of the divalent metal ions.

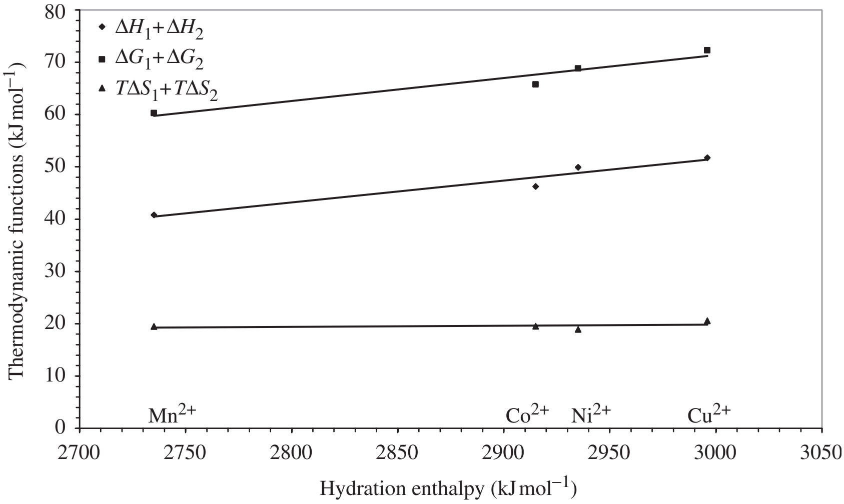

Figure 4. Variation of the overall thermodynamic functions at 308 K for BMHP complexes with the divalent metal ions enthalpy of hydration.

reveals that the most of the BMHP complexes have similar geometry [58]. Moreover, $-\Delta G$ and $-\Delta H$ increase with increasing electronegativity of the metal ion, inconsistent with the fact that increasing electronegativity of the metal ion will decrease the electronegativity difference between the metal ion and the donor atoms of the ligand. Thus, the metal–ligand bond would have more covalent character, which may lead to greater stability (higher $-\Delta G$ and $-\Delta H$ values) of the metal complexes.

Overall $-\Delta G$ and $-\Delta H$, values for the complexation of BMHP with the divalent metal ions follow the order: $Cu^{2+} > Ni^{2+} > Co^{2+} > Mn^{2+}$ in agreement with the Irving–Williams series [59]. This is in line with the fact that the greater the electron acceptor ability of a metal, the stronger will be the complexes that forms and hence, the more negative values of ΔG and ΔH.

It is apparent that the transition metal complexes of BMHP are stabilized, table 6, by both favorable enthalpy (negative values) and entropy (positive values) changes. The relatively small values of $T\Delta S^0$ coupled with large values of ΔH^0 suggest that enthalpy is the main driving force for complex formation in solution.

In general, it is noted that the thermodynamic functions of the Cu^{2+} complex are higher than those of other metal ions. This is due to the extra stabilization exerted by its unique electronic configuration (d^9), which is subject to the Jahn–Teller effect.

Acknowledgements

The authors would like to acknowledge Kuwait University for the provision of grant No. SC04/03 and the general facility projects grant Nos GS0/01 and GS03/01.

References

[1] P.K. Singh, D.N. Kumar. *Spectrochim. Acta A*, **64**, 853 (2006).
[2] J.J. Sha, M.H. Zhang, Y.J. Jiang. *The Handbook of New Breed Pesticide of Overseas*, Chemical Industry Press, Beijing (1993).
[3] R. Gup, B. Kirkan. *Spectrochim. Acta A*, **62**, 1188 (2005).
[4] Q.B. Song, Z.L. Lu, X.L. Wu, Y.X. Ma. *Trans. Metal Chem.*, **19**, 503 (1994).
[5] Z.-L. Lu, C.-Y. Dun, Y.-P. Tian, X.-Z. You, H.-K. Fun, K. Sivakumar. *Acta Crystallogr Sect.*, **52**, 1507 (1996).
[6] A.C. Cunha, J.L.M. Tributino, A.L.P. Miranda, C.A.M. Fraga, E.J. Barreiro. *IL Farmaco*, **57**, 999 (2002).
[7] G. Murineddu, G. Loriga, E. Gavini, A.T. Peana, A.C. Mule, G.A. Pinna. *Arch. Pharm.*, **334**, 393 (2002).
[8] S.K. Sridhar, A. Ramesh. *Biol. Pharm. Bull.*, **24**, 1149 (2001).
[9] B. Kalluraya, A.M. Isloor, P.V. Frank, R.L. Jagadeesha. *Indian Heterocycl. Chem.*, **13**, 245 (2004).
[10] B.A. Booth, E.C. Moore, A.C. Sartorelli. *Cancer Res.*, **31**, 228 (1971).
[11] A. Vamvakides. *Pharm. Fr.*, **48**, 154 (1990).
[12] P.C. Unangst, G.P. Shurum, D.T. Connor, R.D. Dyer, D.J. Schrier. *J. Med. Chem.*, **35**, 3691 (1992).
[13] M.D. Mullican, M.W. Wilson, D.T. Connor, C.R. Kostlan, D.J. Schrier, R.D. Dyer. *J. Med. Chem.*, **36**, 1090 (1993).
[14] D.H. Jones, R. Slack, S. Squires, K.R.H. Wooldridge. *J. Med. Chem.*, **8**, 676 (1965).
[15] J.K. Sughen, T. Yoloye. *Pharm. Acta Helv.*, **58**, 64 (1978).
[16] A. Shams El-Dine, A.A.B. Hazzaa. *Pharmazie.*, **29**, 761 (1974).
[17] T. Misato, K. Ko, Y. Honma, K. Konno, E. Taniyama. JP 77-25028 (A01N 9/12); *Chem. Abstr.*, **87**, 147054a (1977).
[18] A. Cansız, S. Servi, M. Koparır, M. Altıntaş, M. Dığrak. *J. Chem. Soc. Pak.*, **23**, 237 (2001).
[19] M.R. Stillings, A.P. Welbourn, D.S. Walter. *J. Med. Chem.*, **29**, 2280 (1986).
[20] J.M. Kane, M.W. Dudley, S.M. Sorensen, F.P. Miller. *J. Med. Chem.*, **31**, 1253 (1988).
[21] N.A. Al-Awadi, N.M. Shuaib, A. El-Dissouky. *Spectrochim. Acta A*, **65**, 36 (2006).
[22] N.M. Shuaib, N.A. Al-Awadi, A. El-Dissouky, A. Shoeir. *J. Coord. Chem.*, **59**, 743 (2006).
[23] H. Dib, N. Al-Awdi, Y. Ibrahim, O. El-Dusoukui. *J. Phys. Org. Chem.*, **17**, 267 (2004).
[24] G.H. Jeffery, J. Bassett, J. Mendham, R.C. Deney. *Vogel's Textbook of Quantitative Chemical Analysis*, 5th, Longman, London (1989).
[25] T.M. El-Gogary, A. El-Dissouky, A.S. Hilali. *Int. J. Quant. Chem.*, **91**, 685 (2003).
[26] B. Jeragh, A. El-Dissouky. *J. Solution Chem.*, **33**, 427 (2004).
[27] G. Van Uitert, C.G. Hass. *J. Am. Chem. Soc.*, **75**, 451 (1953).
[28] L. Pettit (University of Leeds, U.K), Personal Communication.
[29] W.J. Geary. *Coord. Chem. Rev.*, **7**, 81 (1971).
[30] L.K. Thompson, F.L. Lee, E.J. Gabe. *Inorg. Chem.*, **27**, 39 (1988).
[31] K. Nakamoto. *Infrared and Raman Spectra of Coordination Compounds*, 5th Edn., Part B, John Wiley & Sons, Inc (1997).
[32] R.L. Dutta, A. Symal. *Elements of Magnetochemistry*, 2nd Edn, Affiliated East-West Press, New Delhi (1993).
[33] D.F. Xiang, C.Y. Duan, X.S. Tan, Q.W. Hang, W.X. Tang. *J. Chem. Soc., Dalton Trans.*, 1201 (1998).
[34] T. Mathur, U.S. Ray, J.-C. Liou, J.S. Wu, T.-H. Lu, C. Sinha. *Polyhedron*, **24**, 739 (2005).
[35] A.B.P. Lever. *Inorganic Spectroscopy*, p. 448, Elsevier Science, Amsterdam (1984).
[36] S.H. Oaklay, D.B. Soria, M.P. Coles, P.B. Hitchcock. *Polyhedron*, **25**, 1247 (2006).
[37] F.A. Cotton, C.A. Murillo, D.J. Timmons. *Polyhedron*, **18**, 423 (1999).
[38] A. Sreekanth, M. Joseph, H.-K. Fun, M.R.P. Kurup. *Polyhedron*, **25**, 1408 (2006).
[39] W. linert, F. Renz, R. Boca. *J. Coord. Chem.*, **40**, 293 (1996).
[40] S. Purohit, A.P. Koley, L.S. Prasad, P.T. Manoharan, S. Ghosh. *Inorg. Chem.*, **28**, 375 (1989).
[41] L.J. Bostelaar, R.A.G. deGraaf, F.B. Hulsbergen, J. Reedijk, W.M.H. Sachtler. *Inorg. Chem.*, **23**, 2294 (1984).
[42] A. El-Dissouky. *Spectrochim. Acta, A*, **43**, 1177 (1987).
[43] R. Ruiz, A. Aukauloo, Y. Journaux, I. Frenandez, J.R. Pedro, A.L. Rosello, B. Cervera, I. Castro, M.C. Munoz. *Chem. Commun.*, **989** (1998).
[44] N. Arulsamy, D.J. Hodgson. *Inorg. Chem.*, **33**, 4513 (1994).
[45] S.G. Vulfson. *Molecular Magnetochemistry*, Gordon and Breach Science Pub, Amsterdam (1998).
[46] A. Klanicova, Z. Travnicek, I. Popa, M. Cajan, K. Dolezal. *Polyhedron*, **25**, 1421 (2006).
[47] A. El-Dissouky, G.B. Muhammad. *Inorg. Chim. Acta*, **162**, 263 (1989).
[48] C.A. Otter, S.M. Couchman, C.J. Jeffery, K.L.V. Mann, E. Psillakis, M.D. Ward. *Inorg. Chim. Acta*, **278**, 178 (1998).
[49] H. Irving, H.S. Rossotti. *J. Chem. Soc.*, 3397 (1953).
[50] H. Irving, H.S. Rossotti. *J. Chem. Soc.*, 2904 (1954).

[51] F.I.C. Rossotti, H.S. Rossotti. *Acta Chem. Scand.*, **9**, 1166 (1955).
[52] M.T. Beck, I. Nagybal. *Chemistry of Complex Equilibria*, Wiley (1990).
[53] W.U. Malik, G.D. Tuli, R.D. Madan. *Selected Topics in Inorganic Chemistry*, 3rd Edn, S. Chand & Company Ltd, New Delhi (1984).
[54] H.M. Irving, R.J.P. Williams. *Analyst (London)*, **77**, 813 (1952).
[55] F.R. Harlly, R.M. Burgess, R.M. Alcock. *Solution Equilibria*, p. 257, Ellis Harwood, Chichester (1980).
[56] C.S.G. Phillips, R.J.P. Williams. *Inorganic Chemistry*, Vol. 2, p. 268, Oxford (1966).
[57] A.A. El-Bindary, I. Shehatta, E.M. Mabrouk. *Monatsh, Chem.*, **125**, 373 (1994).
[58] S. Murakami, Y. Yoshino. *J. Inorg. Nucl. Chem.*, **43**, 2070 (1981).
[59] H. Irving, H.S. Rossotti. *J. Chem. Soc.*, 3192 (1953).